University of Virginia Human Powered Vehicle Team
2021 ASME HPVC E-Fest Design Report

Vehicle Name: Smithinator 2.0, Vehicle #11

By:
Ryder Sadler
Joe Flynn
Kavi Patel
Lauren Weis
Riley Roe
Skyler Moon
Trevor Marchhart

Advised By:
Natasha Smith
Sebring Smith

Contact Information:
Team Member Contact: Ryder Sadler (rs2md@virginia.edu), Kavi Patel (kkp5ab@virginia.edu)
Faculty Advisor Contact: Natasha Smith (nls5m@virginia.edu)

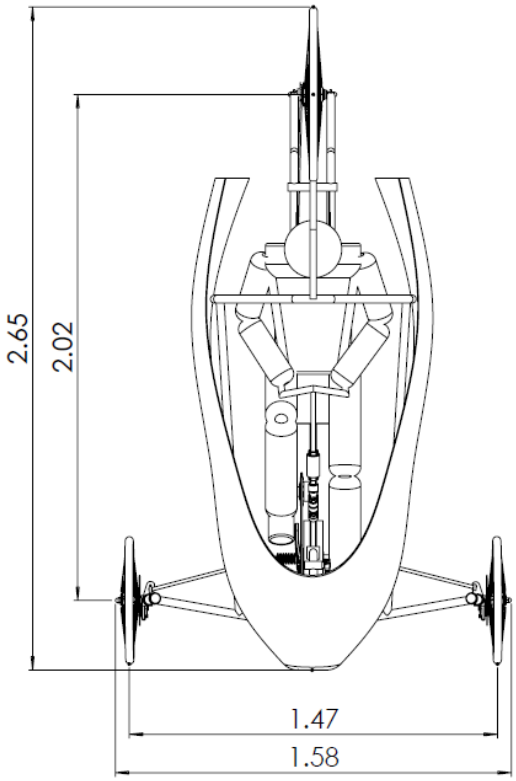

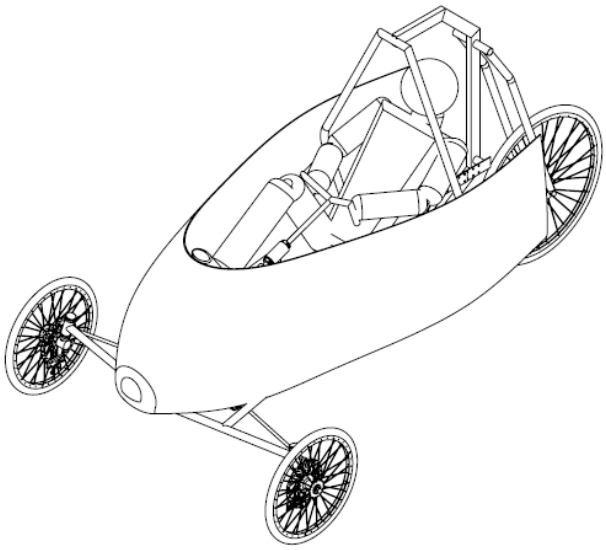

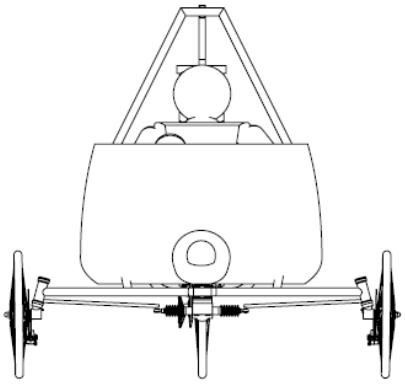

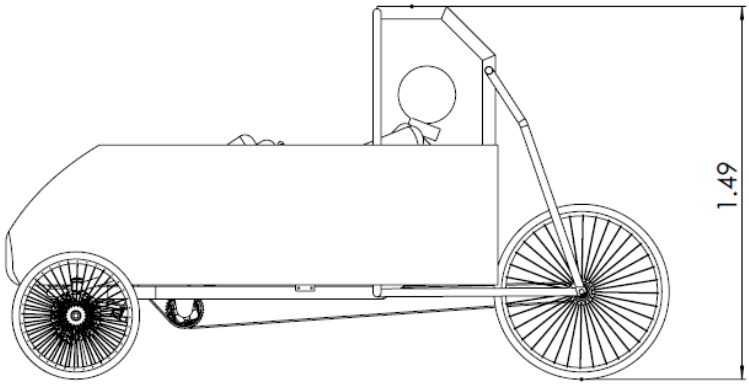

		UNLESS OTHERWISE SPECIFIED:		NAME	DATE
		DIMENSIONS ARE IN INCHES	DRAWN	Trevor M.	4/30/21
		TOLERANCES: FRACTIONAL ± ANGULAR: MACH ± BEND ± TWO PLACE DECIMAL ± THREE PLACE DECIMAL ±	CHECKED		
			ENG APPR.		
			MFG APPR.		
		INTERPRET GEOMETRIC TOLERANCING PER:	Q.A.		
		MATERIAL	COMMENTS:		
NEXT ASSY	USED ON	FINISH			
APPLICATION		DO NOT SCALE DRAWING			

TITLE: UVA HPVC Team

SIZE	DWG. NO.	REV
D	Assembly	4

SCALE: 1:15 WEIGHT: 100lbs SHEET 1 OF 1

Abstract

The University of Virginia Human-Powered Vehicle Team has designed a vehicle to compete in the American Society of Mechanical Engineers Human-Powered Vehicle competition. However, as the competition races were canceled for this year, the team decided to focus on designing a vehicle that could be used as a single-occupant commuter vehicle for urban travel. The team's focus on that particular application is based on an initiative of the city of Charlottesville to reduce single-occupant vehicle gas usage through walking or biking when possible (Albemarle County Board of Supervisors, 2020).

The vehicle is a recumbent tadpole tricycle, with two front wheels and one rear wheel. It is constructed around a central spine built to provide strength while not adding excessive weight to the overall frame. The drivetrain was designed to be efficient at powering the vehicle at sustainable power levels for average humans. The vehicle is powered by a two-chain, rear-wheel-drive system, where the power is transmitted from the pedals to an intermediate gear, then to the rear wheel in order to route the drivetrain around the steering assembly. The vehicle is equipped with a carbon fiber fairing to make the vehicle more aerodynamic. Ackerman steering geometry is integrated with an "off-the-shelf" rack-and-pinion system transmitting the rider input from an over seat steering wheel to the front wheels. As this vehicle is intended to be a commuter vehicle, extra effort was put into removing unnecessary complications from the user interface. The brake controls are one such system. The braking system is installed on the front wheels, in accordance with the competition rules, and is controlled by a single lever on the steering wheel.

Multiple computational tests, such as Finite Element Analysis and Computational Fluid Dynamics, were used to test subsystem concepts, verify design choices, and ensure the vehicle meets the team's design specifications.

Manufacturing of the vehicle took place in Lacy Hall throughout the 2021 Spring semester. The frame was the first subsystem to be built, as all of the other subsystems are dependent upon it. Numerous lessons were learned throughout the manufacturing process, the most important being timing and ordering of subsystem manufacturing.

Table of Contents

1. Design

1.1 Objective

The initial objective of the team was to design, develop, and manufacture a competitive vehicle to compete in the annual HPVC competition with a focus on requirements set by ASME. The ongoing coronavirus pandemic affected the teams' goals when the competition was transitioned to an online-only format with a focus on design and innovation. The team then pivoted to focus on developing a human-powered vehicle that could act as an attractive alternative to traditional combustion methods for short-distance commutes. From this objective, the following design objectives were developed.

The design needed to provide a safe, reliable, and comfortable environment for the rider. The frame was optimized to minimize weight while exceeding the load requirements set by ASME for the Rollover Protection System (RPS) when tested using Finite Element Analysis (FEA) in SolidWorks. Pugh design matrices were used when designing the vehicle subsystems to optimize vehicle performance without sacrificing rider safety. This was to ensure peace of mind for commuters looking to adopt alternative transportation methods.

Second, the design must seek to optimize the performance of the rider such that it can effectively act as a transportation method. Biomechanics research was conducted to maximize the power generation of the rider. Steering and braking were optimized to exceed the

requirements set by ASME for each vehicle concerning turning radius, straight-line stability, and braking. The utilization of an internal hub allows the vehicle to accelerate efficiently from a stop and perform at a high level throughout a range of gearing ratios with minimal losses due to wear and tear associated with external gearing mechanisms. Drivetrain and ergonomic design were developed in parallel to exceed ASME requirements for speed and acceleration. These design objectives contributed to the goal of providing a human-powered vehicle that is feasible for use by short-distance commuters.

Lastly, the team sought to improve the manufacturing skills of the entire team by engaging in hands-on training in welding, turning, and various other general manufacturing techniques. Additionally, HPVC offered an opportunity for students to collaborate, develop, and manufacture a complicated design from scratch while having to adapt to the challenges associated with the ongoing pandemic.

1.2 Background

Our team focused on creating a recumbent vehicle for the competition that can perform as a commuter vehicle. To address the comfort and difficulty issues of biking, our team conducted extensive research relevant to the main “subsystems” of the vehicle. These subsystems are frame, fairing, drivetrain, steering, brakes, and wheels.

A review of the drivetrains of human-powered vehicles created by Cote et. al in 2019 and Fisher et. al in 2015 was conducted to determine common designs. Most recumbent human-powered vehicles were found to be in a delta or tadpole design in which two wheels are in the back or front respectively. Driving a single wheel is the most common way to power the bikes.

The position of the driver is important because it can affect weight distribution. Recumbent or more reclined positions are preferred when retracting your leg towards your body while pedaling because gravity is helping to move the leg along its path. However, one issue with a more reclined or recumbent position is that it is not optimal for hills because most of the weight is shifted to the back of the vehicle (Jong, 2006).

The cadence of the driver is also important to conserve energy based on the gear and the type of cycling being performed, e.g. sprint versus endurance. For a pure speed competition, the highest gear and the fastest pace would be optimal. In an endurance challenge, it is expected that 53-60 rpm is the ideal cadence. This is based on a study conducted by Jong showing the most economical cadence to be that which creates minimized metabolic demand, especially in the gluteus maximus (2006).

Warren Beauchamp is a lifelong recumbent human-powered vehicle competitor and expert who runs recumbents.com, an informative recumbent vehicle website/publication. Recumbents.com introduced many key concepts for the development of the team’s human-powered vehicle including but not limited to caster angles, kingpin inclination, and the location of the steering wheel or the handlebars. The caster angle is the slope of the vertical headstock with respect to the vertical as shown in Figure 1, and a positive caster decreases the prevalence of the car drifting from a straight line when not actively steering. This angle was highlighted by both recumbents.com and in an interview with Basic Cycles, a local bike shop.

The kingpin inclination is the angle of the hub's axis of rotation with respect to vertical as shown in Figure 2. Kingpin inclination is used to control the scrub radius, a lower scrub radius decreases the effort required to steer the vehicle, especially at low speeds (Beauchamp 2018).

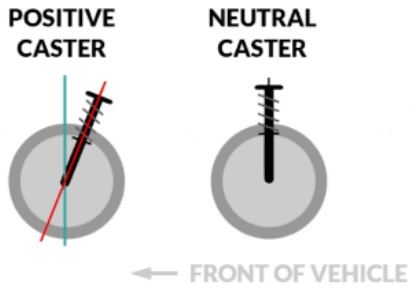

Figure 1: Example of positive caster on a vehicle (LaFranc 2019)

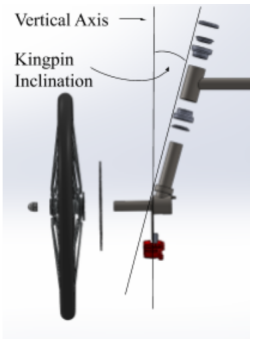

Figure 2: Exploded view of the steering assembly illustrating how the kingpin inclination impacts the design of the wheel assembly

Multiple sources including a professor from the University of Alabama and recumbents.com both highlight Ackermann geometry as the most effective practice when designing common vehicle steering. This is a geometric arrangement of linkages in the steering of a car or other vehicle designed to solve the problem of wheels on the inside and outside of a turn needing to trace out circles of different radii as shown in Figure 3. This is done by having linkages attached to the wheel assembly that traces to the center of the rear axle as shown in Figure 4. The geometry of the frame determines the Ackermann angles and the lengths of linkages and the relevant geometry can be seen in Figure 4.

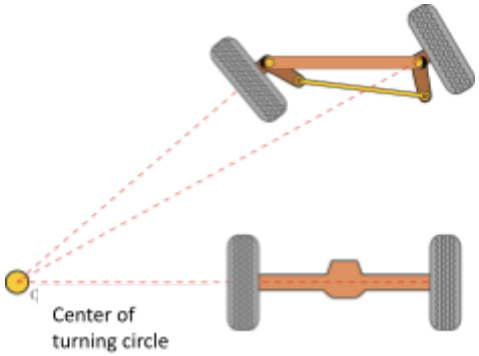

Figure 3. Variable wheel turning radius when rounding a turn

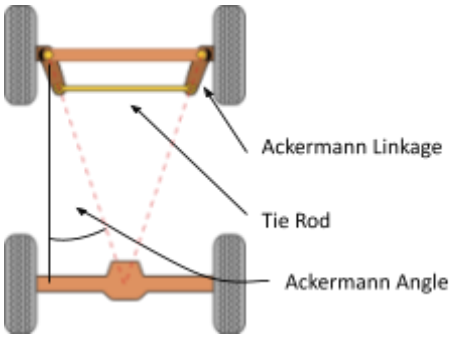

Figure 4. Ackermann angles determined via the length and width of the vehicle

A review of similarly-designed, commercially available recumbent bikes and trikes showed a prevalence of two main types of braking mechanisms: caliper brakes and disc brakes. Caliper brake systems consist of a pair of pads connected by lever arms. The lever arms straddle the wheel and apply pressure to the wheel rim in order to stop the bike. Disc brakes, on the

other hand, require a thin metal disc on the wheel hub that the brake assembly squeezes to stop the vehicle.

As the competition requires a set of brakes on each front wheel, the team's design requires two sets of brakes. One problem with using separate brakes on two wheels is uneven and therefore unpredictable braking; there is a chance the driver applies uneven pressure across the two systems. Commercial solutions to this potential problem involve controlling two brakes with a single lever by splitting the brake line.

1.3 Prior Work

Smithinator 2.0 is a new design but previously established manufacturing techniques, generic steering methodology, and materials were reused. Chromoly 4130 steel was used in the design, 4130 is widely accepted as optimal for the intended use and is not seen as a carryover from previous designs. Accepted steering geometries like utilizing a kingpin inclination or camber angles that impact steering performance are general knowledge in vehicle development and differed from previous year's vehicles. "Lessons Learned" documents from previous teams guided the design process and potential complications the team could face during the design and manufacturing stages. These documents informed strategy and planning but the design remains completely original to this year's team.

1.4 Organizational Timeline

The team began work on the preliminary designs at the beginning of September 2020. The team chose to work with a design that had a strong spine and web. The team then split up into groups to work on frame, biomechanics, fairing, drivetrain, steering, and brakes. The frame team worked from late September until November 2020 on the Finite Element Analysis (FEA). FEA was completed for the competition safety loads, the force from pedaling, and the load from the weight of the driver. The FEA demonstrated that the design had sufficient structural integrity in all locations except for the front crossbeam. This problem was easily solved since the rack and pinion system needed to be moved under the frame, so the design naturally changed. The design shifted again when the tubing sizes were altered, and the FEA again demonstrated that the design was structurally sufficient.

The biomechanics team worked from late September until November 2020 to determine the best angles for the seat, and the distance the pedals should be away from the seat based on the driver's heights. The idea for the fairing came at the end of September when the frame was being developed. However, the fairing was not designed in SolidWorks until January because its design was not essential to the designs of the other components. Preliminary decisions for the drivetrain such as using feet and not hands to pedal and front versus rear-wheel drive were made when the basic design of the frame was chosen. The more specific aspects of the drivetrain were finalized by the end of October 2020. The brake team chose disc brakes over rim brakes and chose specific wheels, rims, spokes, and hubs in late October. All of the component design teams had their ideas implemented into the final design by the end of November 2020. The teams then got together to work on the final design report which was completed in January 2021.

Table 1: Timeline

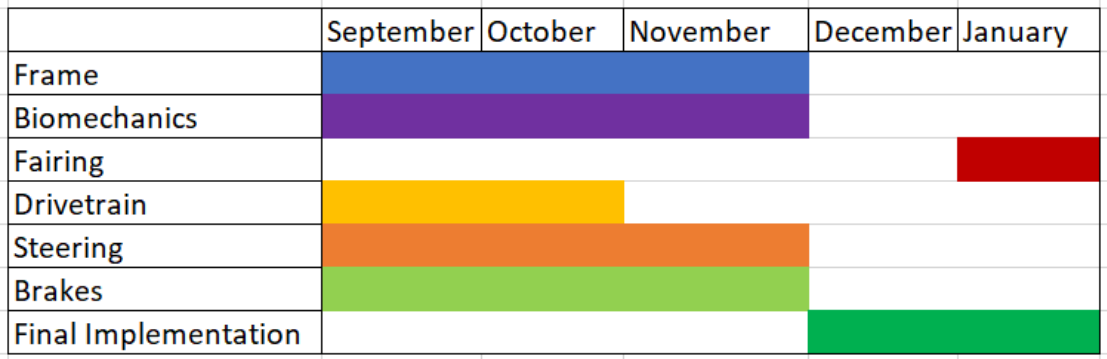

1.5 Design Specifications

Most of the team's initial design specifications were developed from the minimal safety requirements for entrance into the ASME Human-Powered Vehicle Challenge. The subsystems governed most heavily by the safety requirements include the frame, the brakes, and the steering. The maximum acceptable frame deflection was reduced from the ASME required value of 5.1cm to 4cm to minimize the risk of rider injury from a collapsing frame during a crash. A similar approach was also taken for the brake specifications, where the braking distance was shortened to 5m to allow for slower rider reaction times if emergency braking is necessary. The steering turning radius specification was reduced from 8m to less than 6m to allow for increased maneuverability. The team chose design specifications that outperform the competition specifications by an average of 10-20% to increase the factor of safety of the vehicle to account for unforeseen circumstances the vehicle could encounter. Other system specifications were derived from the competition rules. The drivetrain had no specific competition requirements, so the speed from the braking test was adopted as a target low-effort cruising speed. The size of the vehicle was determined from the range of heights of the team members who will pilot the vehicle. The final set of design parameters came from usability and competitive concerns. For example, the weight of the vehicle was not specified by any competition rules, but the team decided on a goal weight of less than 100 lbs to keep the vehicle lightweight. A lightweight vehicle is ideal for commuters because it decreases the amount of work the rider has to do. The quantitative values for the design specifications are summarized in Table 2 below.

Table 2: Design Specifications

Competition Parameter	Parameter Value	Team's Design Specification
Braking Distance	6 meters from ≥25 km/h	5 meters from 25 km/h
Stability	Travels straight 30 meters at 5-8 km/h	Same as competition requirements
Rollover Protection	<5.1 cm of deflection for the top load of 5340N, <3.8 cm of deflection for the side load of 2670 N	<4 cm deflection for top load case, <3 cm for side load case
Turning Radius	8 meters	<6 meters
Weight	N/A	< 100 lbs.

Size	Fits tallest and shortest riders with >2” clearance between helmet and roll cage	Fits riders between 66” and 77” with >2” clearance

Furthermore, some qualitative design specifications were also developed to better enable the use of the vehicle as a commuter vehicle. These specifications mostly centered around comfort and eliminating typical sticking points in human-powered vehicles. To address rider comfort, the team decided the vehicle should be able to be ridden for two hour-long rides with minimal discomfort. A common sticking point for human-powered vehicle users is shifting and getting stuck in an undesirable gear while starting to pedal. The team wanted to ease shifting concerns for the driver by enabling shifting while the vehicle is not in motion.

1.6 Concept Development and Selection

A decision matrix or Pugh matrix is a visual and quantitative methodology to compare possible solutions on key characteristics of the subsystem. The importance column rates the desired characteristic for the subsystem from 1-5. Then the characteristics of potential solutions are rated 1-5 on their ability to successfully meet the key characteristic. The scores are multiplied and summed to create a weighted average and the highest weighted average was the solution. These were utilized throughout the concept development and selection process to compare and contrast different concepts for each subsystem.

1.6.1 Frame

The biggest consideration for the concept development of the frame was whether to implement a central spine or a web design. The central spine design has a primary backbone that supports most of the weight. The web design does not have a primary backbone, and its weight is more evenly distributed. The team considered factors such as ease of implementation, availability of prior work, and weight. The central spine may be easier to implement because the central spine could be bent so fewer parts would have to be welded together. The team found that there was more prior work available for the web design than the central spine. Finally, both the web design and the central spine design came out to be similar weights. As shown by the decision matrix, the central spine design is the better choice given the criteria the team chose to look at.

Table 3: Frame Decision Matrix

	Importance (1-5)	Web (1-5)	Central Spine (1-5)
Ease of Implementation	4	3	5
Light-weight	2	3	3
Availability of Prior Work	3	4	3
Overall Score		30	35

1.6.2 Fairing

The vehicle's fairing helps both the overall aerodynamics of the vehicle and an added layer of safety for the driver. Aerodynamics is a vital component of vehicle design, as it allows the vehicle to reach higher speeds and achieve higher acceleration with less power. This is especially important in human-powered vehicle design, as the primary power supply to the

vehicle comes directly from the driver's legs. The goal of fairing design is to create an outer shell of the vehicle that reduces the drag force acting on the vehicle, while also keeping the fairing as light and functional as possible. As well as this, the fairing design must protect the driver from minor crashes and possible flying debris from other vehicles on the road. Shape type and material were analyzed to design and create a fairing that prioritized aerodynamics, safety, and functionality.

The fairing shape was the first decision made in the overall fairing design. The fairing shape would ultimately influence the overall aerodynamics, cost, and weight of the fairing as a whole. Three shapes were considered for the fairing design: fully-enclosed, semi-enclosed, and a windscreen. These fairing types were assessed by aerodynamic advantage, cost and material use, protection of the driver, and ease of access to the inside of the vehicle. Below is a Pugh Matrix accessing these factors.

Table 4: Fairing Type Decision Matrix

	Importance (1-5)	Fully-Enclosed (1-5)	Semi-Enclosed (1-5)	Windscreen (1-5)
Aerodynamic Advantage	4	5	4	2
Cost	2	1	2	4
Protection of Driver	5	5	4	2
Accessibility	5	1	4	5
Overall Score		52	60	51

Ultimately, the semi-enclosed fairing was chosen for best suiting the criteria stated above. The semi-enclosed fairing provided the best trade-off between a small aerodynamic advantage loss compared to the fully enclosed model while providing good accessibility to the vehicle. Aerodynamics, safety, and accessibility were the biggest factors during the decision process, semi-enclosed far outweighed the other options as it also provides ample accessibility.

Fairing material was also a key decision during the fairing design process. Materials such as carbon fiber, plexiglass, and fiberglass were assessed. Material use was decided based on cost, weight, and ease of use when molding. Below is a Pugh Matrix assessing these factors. Based on the factors considered carbon fiber was chosen as the best material to use for the vehicle's fairing. Although carbon fiber is the most expensive material, the lightweight outweighs the losses from the cost.

Table 5: Fairing Material Decision Matrix

	Importance (1-5)	Carbon Fiber (1-5)	Plexiglass (1-5)	Fiberglass (1-5)
Cost	3	2	4	3
Weight	5	5	2	3
Molding Ease	4	3	3	2
Overall Score		43	34	32

1.6.3 Drivetrain

Preliminary decisions were made as to how power is to be generated as well as how it is transmitted to the mechanical drivetrain. The decision as to whether legs or arms would be used to power the vehicle was fairly obvious because the human leg is typically more powerful than the arms. This led to the decision to use pedals because they enable the full extension of the human leg to generate the most power. In a biomechanics paper by Too in 1993, it was found that the pedals should be located at a distance of 90 to 110 percent of the driver's leg, their hip angle should be 100 to 110 degrees from their torso, and the driver should be in the most comfortable position to not waste muscle energy. Driving from the front wheel would require a delta tricycle frame or a mechanism to drive a front axle. Driving a single front axle was deemed more difficult than adapting biking equipment for a single wheel drive. Not only were there driver concerns, but there were concerns over how much the chain system might have to move during a front-wheel turn. Ultimately, the rear-wheel-drive was chosen as the final drivetrain implementation.

Rear-wheel drive raises issues due to how the chain must be routed from the front pedals all the way to the back. Discussions with bike maintenance experts resulted in a two-chain design system. The pedals connect to an intermediate gearset through one chain and a second chain routes from there to the rear wheel.

The three main gearing systems considered were mechanical, electrical, and internal hub gearing systems. Mechanical derailleurs are one of the most common gearing systems used on bikes and they are widely available for purchase. A 12-speed cassette is leftover from last year's human-powered vehicle team, thus making this system free for our team. The electrical system is another semi-common gearing system. Electrical systems still rely on mechanical aspects, but the derailleur, the mechanism responsible for shifting gears, is electronic. The simpler mechanical derailleur is much easier to fix compared to the electrical system, in the case of circuit failure. If the electrical aspect were to fail in a race situation, then the driver would be stuck because it would be too difficult to repair circuitry. This scenario is uncommon, but it must be considered. Furthermore, electrical gearing systems are more expensive than mechanical systems. A decision matrix is shown in Table 6 below to better illustrate the process that went into picking the final gearing system for the drivetrain.

The internal hub system is a closed-in electrical system that resides on the whole wheel that drives the vehicle. Internal hubs resist wear to shifting mechanisms better than traditional mechanical and electrical systems because the moving parts responsible for shifting are enclosed in a sealed unit. Neither the electrical or mechanical systems can shift gears while stopped, but that is a key feature of internal hubs. The internal hub does make it more difficult to change tires since the whole wheel is part of the hub. The internal hub can be the most expensive system, but it is also the most reliable. The internal hub system was chosen because of its reliability and its ability to shift gears while the vehicle is stationary, which will make it much easier for the driver to get the vehicle moving. Furthermore, a gearing analysis was conducted in section 2.5.1 on the internal hub, sprocket, and chainring setup to determine if the vehicle would meet speed standards.

Table 6: Decision Matrix for Drivetrain Gearing System

	Importance (1-5)	Mechanical Derailleur (1-5)	Electrical (1-5)	Internal Hub (1-5)
Ease of Use for Driver	4	2	3	4
Reliability	5	2	4	5
Cost	3	5	3	3
Maintenance	2	3	4	4
Integration	3	4	4	3
Overall Score		51	61	67

1.6.4 Steering

Steering choices that were considered were over-seat steering or traditional steering that would potentially be found in a “go-kart” or car where the hands are placed in front of the chest on a steering wheel with a steering shaft between the rider’s legs connected to a rack and pinion assembly. Turning the steering wheel would yield a linear movement of the rack and pinion assembly that would turn the two front wheels. The alternative is below-seat steering where a rider's hands would be positioned near the hip. The steering would utilize a series of tracks and levers to translate a push and pull motion by the rider into the movement of the wheels. The over-seat steering would be easier to implement and provide a more “familiar” feel for a potential rider. By utilizing an “off-the-rack” rack and pinion assembly also decreases the chance of failure of the system and increases the attractiveness of such a system for the casual user.

Table 7: Decision Matrix for Steering System

	Importance (1-5)	Under-seat steering(1-5)	Over-seat steering (1-5)
Integration	2	4	4
Ease of Use	4	2	4
Safety	4	4	3
Reliability	5	3	5
Overall Score		50	61

To incorporate the various necessary steering angles, Ackermann geometry, and the rack and pinion assembly a front split axle was the optimal solution. A split axle is where the two front wheels are not on the same axle but two independent axles for each wheel. This enables the wheels to move freely from the other which is necessary for Ackermann geometry but makes braking more difficult which will be discussed later in this paper.

Each front wheel needs to include the head tube that the wheels pivot on, the axle for the wheel, the Ackermann linkage that pivots the wheels, and the attachment point for the brakes. When designing this wheel assembly, the team needed the geometries that affect performance. These include the toe angles and the caster angle as well as the use of a kingpin inclination. The kingpin inclination is the angle of the hub's axis of rotation with respect to vertical as shown in Figure 7. Kingpin inclination is used to control the scrub radius, which is the radius of the arc made by the tire's contact patch as it rotates about the axis of the knuckle. A lower scrub radius decreases the effort required to steer the vehicle, especially at low speeds. The competition required a turning radius of >8 meters and the inclusion of a kingpin inclination would decrease the effort required by the driver to turn the rack and pinion assembly and achieve the stated design specifications. The caster is integrated with the frame and improves straight-line performance. The design specifications require straight-line stability at a "cruising speed" of 5-8 km/h and an increased caster would decrease the drift of the vehicle.

1.6.5 Brakes and Wheels

The vehicle's braking system is vital to driver safety. For that reason, the ASME Human-powered Vehicle Challenge specified a braking distance of six meters from a speed of at least 25 kilometers per hour as a requirement for entering the vehicle in the competition. This specification served as the initial design goal for the team, but to ensure the vehicle would meet the competition specifications, the team reduced the braking distance to a more stringent five meters from the same speed.

Disc brakes were chosen over rim brakes for their more consistent braking experience across a wider variety of conditions, a valuable feature for a potential commuter vehicle. Additionally, disc brakes are easier to install on the front wheels because the brake clamps can be attached directly to the bottom of the wheel assembly allowing the brake clamps to stay aligned with the discs and the wheels during steering.

Another consideration for the design of the brake system was the brake controls. Because the vehicle has two front wheels, equal braking force must be applied to both to provide the driver with a predictable braking feel. Because of the competition's requirement of front-wheel braking and the team's choice of two front wheels, two separate braking mechanisms must be used. Traditionally, two separate brake systems require two separate brake levers, but brake splitters allow for one lever to control two brakes and apply an equal braking force to each. Two potential brake splitters were assessed: a hydraulic brake line splitter and a mechanical brake cable doubler. The benefits of the hydraulic splitter include reduced weight, less frequent mechanical maintenance, and self-equalized brake pressure; however, the hydraulic brake lines can develop air bubbles which lessens their braking ability. Conversely, the mechanical cable splitter allows for easier maintenance, easier installation, and a lower overall cost. After consulting bike repair shop owners, the mechanical splitter was selected, primarily for easier installation and maintenance. In order to perform optimally, the mechanical cable splitter only requires the brake cables to be well-lubricated, a task much easier than removing air bubbles from the hydraulic lines. The final cable splitter choice can be seen below. The brake system components were selected based on the design matrix below.

Table 8: Decision Matrix for Brake System

	Importance (1-5)	Caliper Brakes (1-5)	Mechanical Disc Brakes (1-5)	Hydraulic Disc Brakes (1-5)
Ease of Installation on Turning Wheels	4	1	4	4
Braking ability	5	3	5	5
Ease of Maintenance	2	5	4	2
Reliability	5	3	5	4
Cable Splitter usage	3	2	4	3
Overall Score		50	86	74

The wheel system consists of the tires, rims, spokes, and hubs of each wheel, and is significantly tied to the brake system, the steering system, and the drivetrain system. A larger wheel (20” for the front and 27.5” for the rear) was chosen for the rear wheel in order to provide better traction during acceleration. Commuter tires were chosen for this vehicle because they offer a good tradeoff between cushion, traction, and weight, and are therefore ideal for urban HPVs. Because this vehicle is meant primarily for road travel, extra traction to the degree that would be afforded by a mountain bike tire is not needed. However, the tires should be able to handle well in all weather conditions, unlike road bike tires. The thin tires seen on road bikes also provide little to no protection from uneven terrain that might be encountered during travel. The wheel type decision was aided by the design matrix seen in Table 9. The front-wheel hubs, spokes, and rims were selected to fit with the decision to use disc brakes. The rear wheel initially was chosen based on the desired gear ratio specified by the drivetrain subsystem team, but it has since been replaced by a wheel with an internal shifting hub, described in the Subsystem Drivetrain section. The front wheel assembly with the disc brake assembly can be seen below.

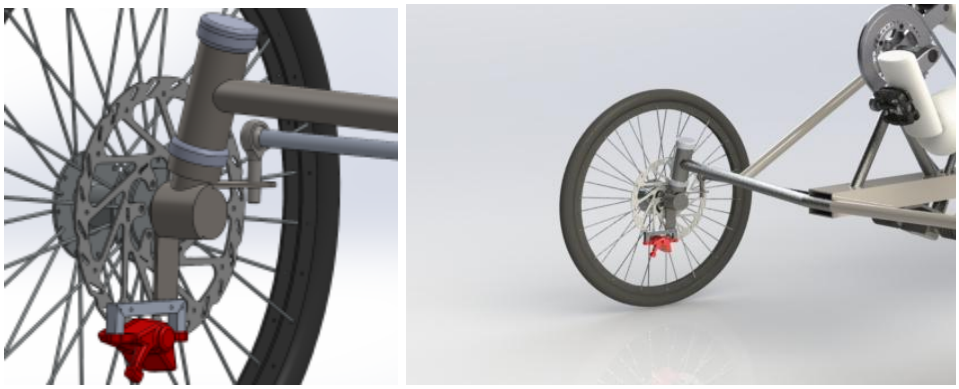

Figure 5. The front-wheel brake assembly mounted on the steering head.

Table 9: Decision Matrix for Wheel and Tire Type

	Importance (1-5)	Mountain (1-5)	Road (1-5)	Commuter (1-5)
Traction	3	4	1	3
Weight	2	1	4	4
Toughness	3	3	1	3
Overall Score		23	14	26

1.7 *Description*

1.7.1 Frame

The frame for the Smithinator 2.0, as shown in Figure 6, is designed with a central spine that runs the length of the vehicle, and wraps around over the top to form the roll cage. The crossbar assembly in the front sits below the central spine to avoid interference with the pedaling. The seat is adjustable and slides along an angled flange, optimized for riders of heights 5'6" to 6'6". In a clinical biomechanics study, Gregor (2002) concluded that for the best power generation, it is important to have the driver seated around 75 degrees from the pedals at a length from 90 to 110 percent of their leg. Biomechanics and frame subsystem teams worked to ensure the adjustable seat could be adjusted for optimal power generation.

Figure 6. Final frame design

1.7.2 Fairing

The fairing is a full carbon fiber design to improve vehicle performance and efficiency and allow for clear visibility. The fairing is enclosed around the bottom of the frame of the vehicle with an opening on the top side for accessibility. The fairing's rounded design allows for maximum aerodynamic advantage to reduce drag without compromising accessibility and visibility. The semi-enclosed design also helps protect the driver from most debris on the roadways while still providing easy access to the inside of the vehicle. The fairing was designed to fit around the frame bottom to provide maximum coverage. The fairing was also designed in a rounded and flowing shape to reduce high-pressure areas. These high-pressure areas caused the most significant increase in drag when examining alternate fairing designs. The design prioritized the comfort of the rider by allowing ample space for limb movements. Ultimately, the fairing was prioritized to fit the frame while minimizing material use and optimizing the aerodynamic advantage for the system.

1.7.3 Drivetrain

The vehicle will be driven by a single rear wheel that is powered by the legs of the driver. The drivetrain will use a two-chain connection system to route the chain from the front chainring to the 27.5 inch rear wheel 8-speed internal hub. The chosen internal hub is a Shimano SG-7001-8 Alfine 8 Speed Rear Hub. This hub can be equipped with a sprocket size of 16T at a minimum and that has been selected for the chain system. ⅛ in chain is one of the

usable sizes for this sprocket, so it was chosen because it is a fairly common spacing and there was a good deal left over from previous bikes. A chain will be routed straight down from the pedals to the first step in a gear train. A second chain would be connected to this first chain through a bracketed set of gears and then connected to the back wheel. The two-chain system allows for straight paths through which the chains will travel, which results in easier modes of maintaining chain tension. The chainring will be a 38T size based on the gearing analysis done by the team and the fact that last year's vehicle had leftover parts for this same chainring. A detailed gearing and power analysis can be found below in section 2.5.2. Furthermore, The

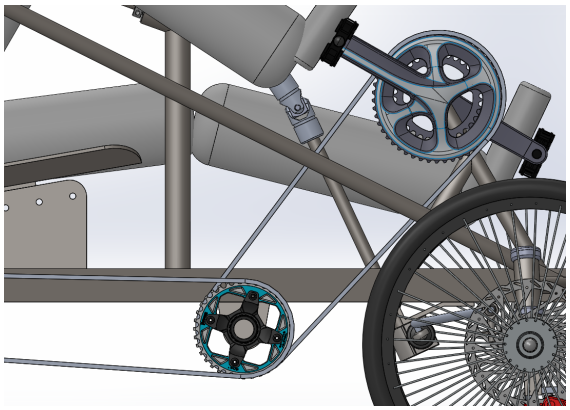

pedal arms for the chainring are 170 mm in length, from last year's vehicle design.

Figure 7. Crankshaft and two-chain assembly junction point for the drivetrain. Some parts are not finalized in the model, but the sizing is accurate.

1.7.4 Steering

An over-seat steering method will be utilized for its ease-of-use for a first-time rider. The "off-the-shelf" rack and pinion assembly will be utilized by the team to deliver a durable, reliable solution for steering that will be able to withstand rain, mud, or dirt. Ackermann steering geometry will be utilized by the team to prevent tire slip when turning. A kingpin inclination (15^{o}), as shown in Figure 8(b), helps to reduce the scrub radius making turning easier for the rider. The wheels will have a positive caster of 2.5^{o}, 0^{o} of camber, and a 15^{o} kingpin inclination as shown in Figures 8. Caster promotes straight-line direction by promoting steering wheel self-centering.

The axle that the front wheels will turn about will be machined from stock 4140 steel rods down to the necessary thickness that passes the FEA conducted by the team but is also easily integrated into the team's chosen "off-the-shelf" wheel. Chromoly 4140 steel is popular for structural tubing, Baja SAE racing, and bicycles for its toughness, high fatigue strength, and impact resistance making it highly suitable for an HPV application. The steering design choices all stem from the objective to make a reliable and accessible human-powered alternative to traditional transportation methods.

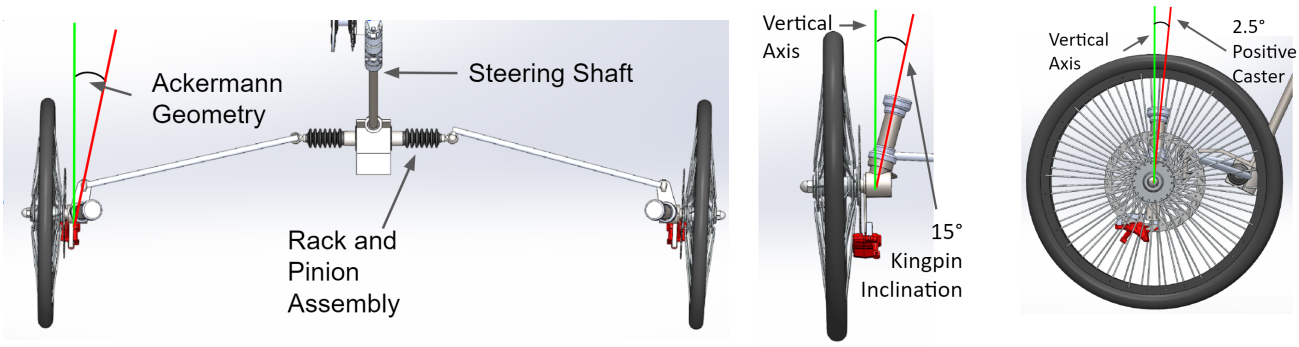

Figure 8: (from left to right) (a) Top down view of the complete steering assembly and the Ackermann geometry angle that is used for steering. The remainder of the vehicle/frame is not pictured and would be above the cutoff of the image, (b) Front view to show kingpin inclination, (c) Side view of the wheel to show the positive caster of the wheel assembly

1.7.5 Brakes and Wheels

The vehicle utilizes disc brakes on each of the front wheels that are controlled by a cable splitter. Disc brakes were chosen to maximize braking ability and reliability. Disc brakes are also relatively easy to maintain and repair, and replacement parts are more widely available than those of other brake types. The mechanical brake cable splitter was selected to simplify the user interface by reducing the number of levers on the steering wheel. A mechanical system was chosen of similar hydraulic systems for installation and maintenance concerns, as the lubrication of a cable was deemed easier than repairing hydraulic lines.

The vehicle is equipped with three commuter bike tires. These tires afford substantial traction on roads in most conditions while not adding excessive weight to the overall vehicle. The front wheels are 20” in diameter and the rear wheel is 27.5” in diameter. The larger back wheel was chosen to provide more traction, which is helpful when the vehicle is accelerating.

1.8 Manufacturing

1.8.1 Frame Manufacturing

The manufacturing process of the frame led to some changes in the design that were not anticipated earlier on. We found that the availability of metal tubing in the shop drove the final selection of sizing for the frame. We had large quantities of 1.25” OD tubes in stock, despite originally designing for 1” OD tubes (see section 2.1). We ultimately chose the larger pipe, as it barely changed the weight and was more convenient. We found that small changes in the design in order to minimize costs and time of manufacturing were usually considered worth it. Additionally, ease of welding was very important during manufacturing, and as a result a few aspects of the design were changed in order to accommodate for easier and stronger welds. For example, the plates welded on to the back end of the frame to secure the internal hub’s shaft

were originally designed to slot into the ends of the tubes. However, we found that it was much easier to weld and much more secure to weld the plates to the side of the tubes, with a gap to allow for solder to form.

The manufacturing process involved utilizing machines such as a pipe bender, a bandsaw, Metal Inert Gas (MIG) and Tungsten Inert Gas (TIG) welding machines, a pipe notcher, and a water jet. The team began by manufacturing the central spine and then building outwards starting with the roll cage. This was for convenience and to ensure that the design for the most central parts of the vehicle would not need to be altered at any point. The frame was welded mainly using TIG welding with MIG welding used for some of the tacking. Medium-density fibreboard (MDF) was cut using a water jet and was used to hold the pipe steady so that there would not be warping due to welding. A pipe notcher was used to notch the pipes at the correct angles and a bandsaw was used for all flat cuts. The roll cage consisted of several pipe bends which allowed for fewer welds. However, the pipe bender was not as precise as the team had anticipated and therefore a few frame adjustments had to be made. The manufacturing of the frame also included working with other subsystems such as wheels and brakes, drivetrain, and biomechanics. For example, the frame team cut and welded a steering shaft and pipes to hold up the pedals and worked with the other subsystem teams to verify their placement before fully welding them on.

1.8.2 Fairing Manufacturing

The manufacturing of the fairing added changes to the overall design of the original fairing more than what was originally expected. Before the manufacturing process, the fairing was designed to optimize the aerodynamic advantage of the vehicle. Very little was considered about the feasibility of manufacturing. Since there was little time at the end of the semester and little expertise in the molding process, the fairing design was simplified. The new design still optimized aerodynamic advantage, but is much smaller and more feasible to create. The design still prioritized the safety of the user and made the overall fairing a lot lighter.

The overall manufacturing process is still occurring at the moment. First, a male mold was designed inside the fairing using solidworks. Originally, the team planned to create a male mold to create a female mold to then mold the carbon fiber for better structural support of the mold. After further research and expert advice, it was determined that because of the shape we were molding, this would be another unnecessary step. The mold was split into two inch thick slices and cut down the middle for sectioning purposes. Rigid insulation foam was purchased and brought to the Architecture School at UVa to be cut by precision cutting and drilling machinery. The cut foam is then glued together into its two separate halves. The separated halves are then cut down and sanded into a smooth curve that fits the exact fairing design. After the male mold has been left to dry, the molding process is ready. A vacuum bag, rope (for air and epoxy flow), peel-ply, carbon fiber layers, shrink wrap, and the male mold are layered in that specific order. Epoxy is injected into the vacuum bag and rope. The system is placed under a constant vacuum until dry and solid. This process is repeated until the fairing is rigid and sturdy. After being left to cure, the fairing is ready for use and testing.

Multiple lessons were learned during the design and manufacturing processes. The most vital lesson learned came from the consequences of not designing the fairing in parallel with the frame design. A suggestion for future teams would be to first come with a set and feasible fairing type. After this, design the fairing with parameters and dimensions that can be easily edited with the adjustment of the frame. The frame was an ever changing entity. Our team waited until the frame design was finalized to design the fairing. Future teams should design then both in tandem to create the most effective design in a safe timeline.

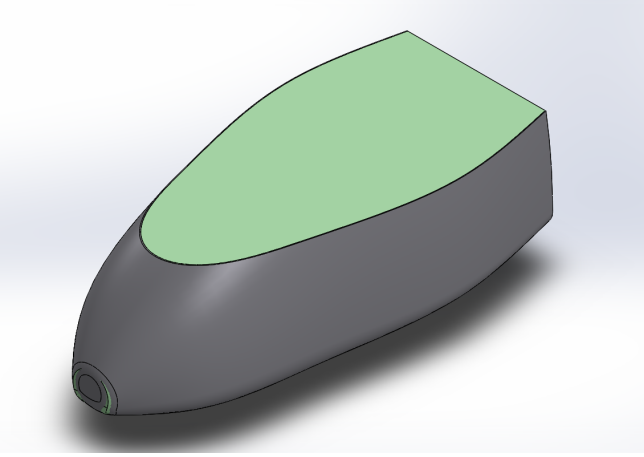

Figure 9: Fairing design over the male mold model

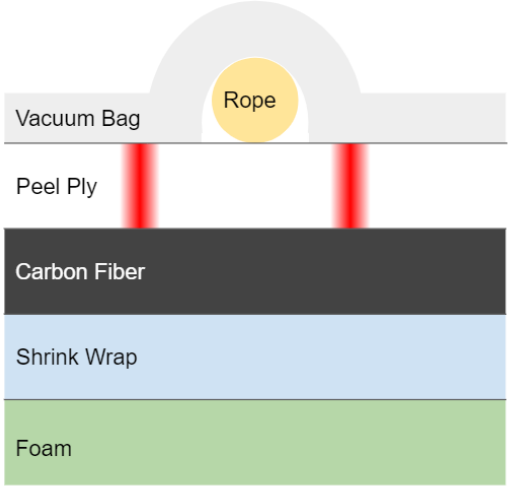

Figure 10: Layered materials in correct order during the molding process

1.8.3 Drivetrain Manufacturing

Manufacturing added changes to the drivetrain beyond what the design process expected. The creation of the interstitial gear to route the chain to the rear wheel required several innovative ideas. The rest of the parts were straightforward and could be bought and applied as they were. The interstitial gear was created using a sealed cartridge bottom bracket

that was suggested by Peloton as the easiest way to meet our needs. The original plan was to weld sprockets onto the bottom bracket but Sebring advised against that method because it may damage the bearings. This was remedied through a series of spacers, washers, and bolts that could hold the sprockets in place. Furthermore, a frame piece was purchased to hold the gear completely still and that piece was welded to the bike for the best connection to the bike. The frame piece works by threading the outside of the bottom bracket into the inside of the frame tubing. From there, the entire gear was fitted into holders that were made by the water jet, and then welded to the vehicle.

Another aspect of the chain system that had to be adjusted was the second half of the chain system. The length of the second chain is much longer than a normal bike chain, thus it requires a tensioner to keep the chain as tight as possible. This was not planned for, but the tensioner is necessary to ensure the chain does not rub or slip on its path to the rear wheel.

Beyond these additions, the internal hub was purchased and put together on the rear wheel with the help of Peloton. The hub came with both a 16T and a 22T sprocket, the latter being on the wheel currently. Furthermore, two 22T sprockets are in place on each side of the interstitial gear. The chainring is a size 32T, but there is also a 38T that can be implemented with a few tweaks to the chain size. The current gear ratios will work based on the detailed gear analysis.

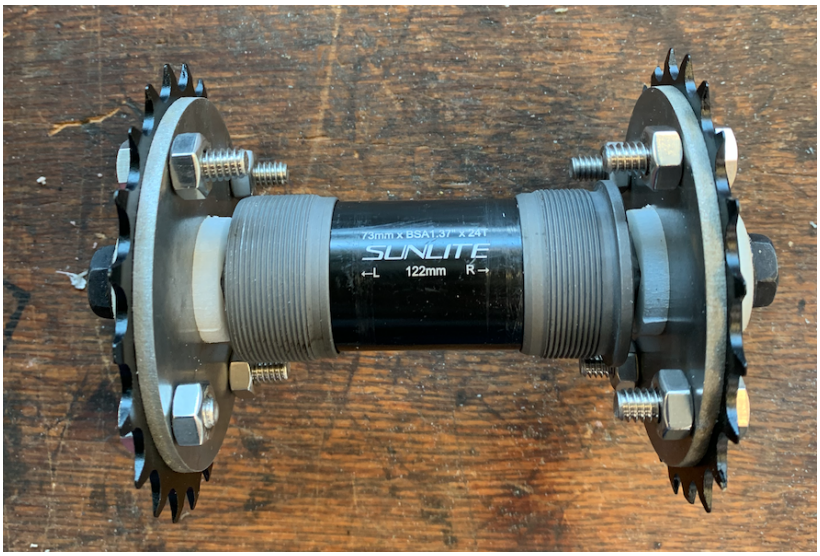

Figure 11: Interstitial Gear before being threaded into its framing.

Figure 12: Front half of two-chain system and the 32T chainring.

1.8.4 Steering Manufacturing

Manufacturing of the steering involved two critical areas of design, the head tube assembly the wheels and brakes rest on and the steering shaft that translates the movement of the steering wheel to the rack and pinion.

Manufacturing of the head tube assembly stayed true to a majority of the design choices including the utilization of a kingpin inclination, positive caster, and Ackermann steering. The manufacturing however proved to be a difficult process due to the specificity needed when pipe-notching these sections. The cantilevered axle that the wheel rests on was from a solid stock tube of steel turned down on a lathe to fit in the wheels bearing. The stock steel then had ⅛" 4130 plates welded to it that had been water jetted out to create the ackermann angles and the attachment point for the disc brakes. The use of solid stock steel and ⅛" steel plates could be a potential area where the vehicle is "overbuilt" or rather significant weight for excessive strength. FEA analysis should be performed based on vehicle weight and forces experienced to potentially reduce the weight of this assembly. When welding the head tube assembly the metal is prone to expansion and consequently changing the angles you have used for the steering geometries. To combat this MIG was used to get an initial tack before exposing to lots of heat when doing the final TIG weld.

There were concerns prior to manufacturing that the steering shaft would have a periodic nature of rotation translation due to the use of U-joints. However the support for the

steering enables the u-joints to be within their working angles laid out by the manufacturer and thus the translation of the rack and pinion was linear and predictable. The rack and pinion used by the team to turn the wheels performed as intended when the steel tie rods were connected to the Ackermann geometry.

Steering manufacturing required close collaboration with the brakes and wheels, biomechanics, frame, and drivetrain systems in order to function properly. Collaboration, open communication, and online video conferencing to effectively manufacture the system in a COVID safe manner.

1.8.5 Brakes and Wheels Manufacturing

Many of the lessons learned in designing and implementing the brake system revolved around the integration of the brakes with the vehicle. One such lesson was that disc brakes are really only designed to be mounted on one side of a bike wheel, typically the left. This means that for a tadpole trike (two wheels in the front and one in the back), both the brake caliper mounting and cable routing for the other disc brake can quickly get complicated. In a tadpole trike configuration, both front wheels are required by the ASME HPVC to be equipped with brakes, so this problem is only avoidable by using a different vehicle configuration or braking system. Another lesson came in developing the interface for controlling the brakes. The biggest challenge for this part of the design came in finding or creating a steering wheel or handlebars that would both fit the brake lever and not obstruct the rider entering and exiting the vehicle. This requires close collaboration with the steering and drivetrain subsystem teams to ensure a design is reached that satisfies the requirements of all three subsystems.

Design and manufacturing of the brakes and wheels subsystem required a great amount of collaboration with the steering team. Because the vehicle is steered by its front wheels and the necessity of front-wheel braking, the brakes had to be mounted in such a way that they would stay aligned with the wheels while the vehicle turns. Ultimately for this vehicle, this was accomplished by mounting the brakes to the steering head. Care was taken to ensure that the brake mounts did not affect the steering. Another area of collaboration with the steering team was the user controls. The brake lever or levers chosen needed to fit the steering wheel or handlebars selected by the steering subsystem team. Work with the drivetrain team was also necessary to select a rear wheel that could accommodate the internal hub.

1.8.6 Biomechanics/Seat Manufacturing

During manufacturing, the height and leg length measurements taken at the beginning of the design process were crucial for seat placement and installation. In addition, design choices such as a rotatable seat and telescoping piping had to be altered for practicality reasons. The seat's adjustability will now involve only translation as well as flush sheet metal plates as the adjustable mechanism.

2. Analysis

2.1 RPS Analysis

The goal of the RPS analysis was to verify the safety of the rider in the case of a vehicle rollover, and optimize the strength/weight of the vehicle. Other factors, such as debris from a crash, can affect the rider's safety. However, the strength of the roll-cage is the primary factor in protecting the rider. The team used SolidWorks FEA to analyze the effect of the two RPS load cases described in the rules. The frame model was designed with the SolidWorks weldments feature, which allowed the elements to be analyzed as beams. When meshing, beams are broken up into a straight line of elements evenly distributed, then results are calculated using the moments of inertia of the cross-section.

For these simulations, the mesh contained 426 beam elements. The fixtures holding the frame were held at the beam joints closest to where the seat would be mounted on the frame. The first load case consisted of a 2670N force applied downward and back 12 degrees from the vertical to the top of the roll cage. The second load case consisted of a compressive side load of 1330N. In order to satisfy the safety requirements of the competition, these loads were not to induce elastic deformations of 51mm and 38mm, respectively, or inelastic deformation anywhere on the vehicle.

The first design iteration used 4130 steel 3/4 S40 pipe, which had an OD of 1.050" and a wall thickness of 0.113", as well as a 3x2", 0.25" thick rectangular central spine. This initial model weighed over 160lbs, so it had to be reduced to meet the design specification of weighing <100lbs. After conducting FEA, it was found that the largest displacements were less than 20% of the allowed maximum, confirming that the frame structure could be safely thinned. The next design used the same material, but a tube with 1" OD, 0.065" wall thickness, and 3x2", 0.125" thick rectangular central spine. This iteration met our design specification of keeping the overall weight under 100lb, with the frame coming in at a weight of 70lbs. The maximum displacements of this design remained well below the allowed elastic deformations of 51mm and 38mm, respectively. Additionally, both load cases kept the upper bound of the stresses significantly below the yield strength of the material. However, in the early planning stages of manufacturing, we found that this design was still much heavier and stronger than we needed. As a result, we again reduced the central spine to a 1x2", 0.125" thick rectangular channel. The pipe sizes were actually increased to 1.25" OD, 0.065" wall thickness tube, as we had large amounts of this size leftover from last year's team. Figures 9 and 10 respectively show the displacement and stress plots of the top load and side load cases for the final design. Factors of safety were calculated for both load cases by dividing the yield strength by the maximum axial and bending stress. These came out to 3.28 and 2.96, respectively. This led the team to conclude that the vehicle was safe enough.

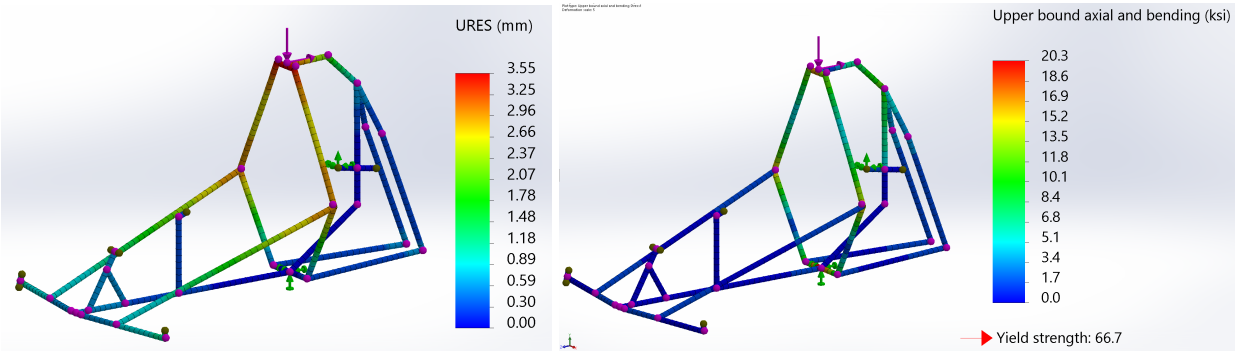

Figure 13. Top load case resultant displacement and upper bound stress plots (final design)

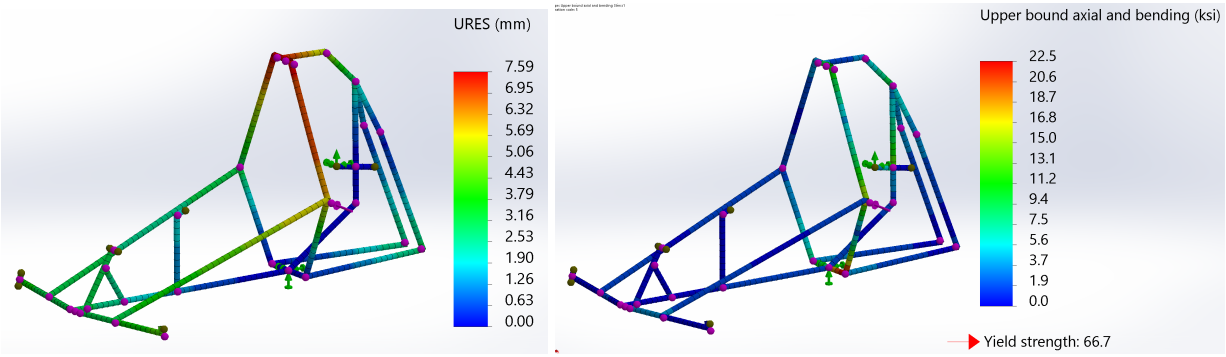

Figure 14. Side load case resultant displacement and upper bound stress plots (final design)

2.2 *Structural Analysis*

For the other structural analysis conducted on the frame, the team used FEA again to analyze the pedaling force and the load from the weight of the driver. For the purpose of this analysis, a pedaling force of 2000N was used which was derived from the weight of the driver. This assumes the rider is not accelerating upwards or downwards. If the average force of an 80kg rider is 800N, then the maximum can be described by twice that, 1600N. However, a cyclist can pull down on the handlebars, or in the case of a recumbent tricycle, push on the back of the seat. This can increase the maximum force. The estimated maximum pedaling force on one pedal was thus estimated to be 2000N. The setup for this FEA was similar to the RPS analysis, except the mesh was refined at the crankshaft and the crankshaft support. This increased the number of elements to 473. Additionally, the 2000N pedaling force was directed at the end of one side of the crankshaft, pointing towards the front of the vehicle. A displacement of 6.00 mm was found at the front crossbar of the vehicle and a stress of about 39.1 ksi was found on the beam holding the pedals (Figure 11). This is significantly under the yield strength of 66.7 ksi. The effect of the force of gravity and the weight of the rider (estimated 800N) were analyzed next. The FEA was set up similarly to the RPS analysis here as well, except the weight force was directed downward at the base of the seat, gravity was applied to the whole simulation, and the model fixtures were placed at the wheel axes. The maximum displacement was at the top of the vehicle at about 2.66 mm, and the maximum stress was found at the ends of the front crossbar near the wheels at 11.4 ksi (Figure 12). Again, this is significantly less than the yield strength of 66.7 ksi. Factors of safety were calculated for this analysis in the same manner as the RPS analysis. These came out to 1.71 and 5.85, respectively. This led the team to conclude that the vehicle was safe regarding pedaling force and weight load.

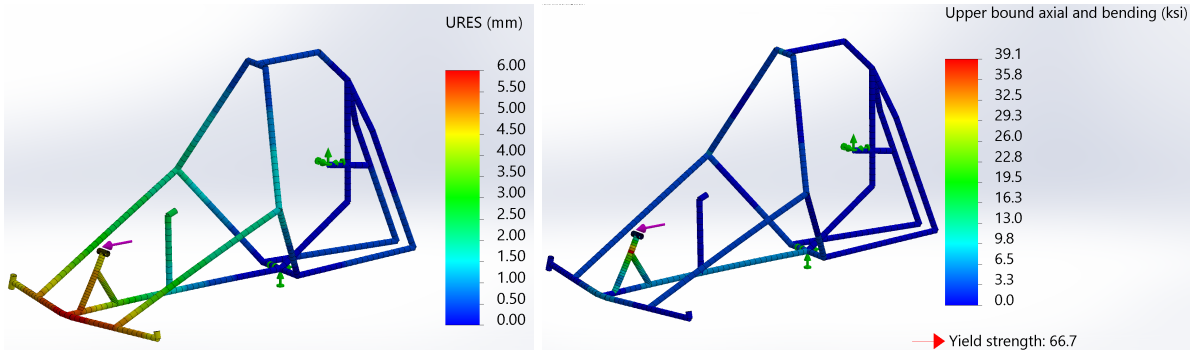

Figure 15. Pedaling force resultant displacement and upper bound stress plots

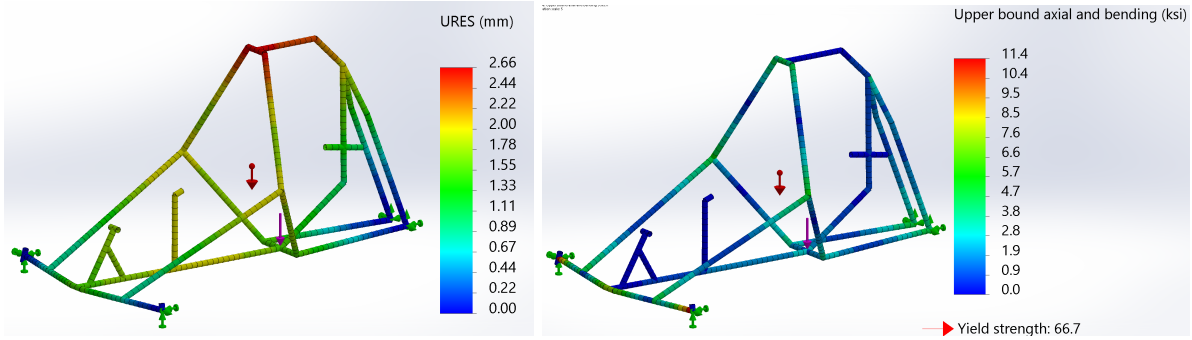

Figure 16. Gravity and rider weight resultant displacement and upper bound stress plots

2.3 Aerodynamic Analyses

For aerodynamic analysis, Computational Fluid Dynamics (CFD) was used. CFD was used to assess the preliminary design of the fairing. Using 3D computer software, airstreams were simulated on both the vehicle with and without a fairing to determine the drag force on the vehicle. Air properties such as temperature and pressure were held constant in both scenarios to get an accurate comparison. A moving velocity of 15 m/s was also set as an initial condition for both scenarios. Flow trajectories over the vehicle with and without a fairing under these initial conditions and velocity vectors can be seen in figure 13.

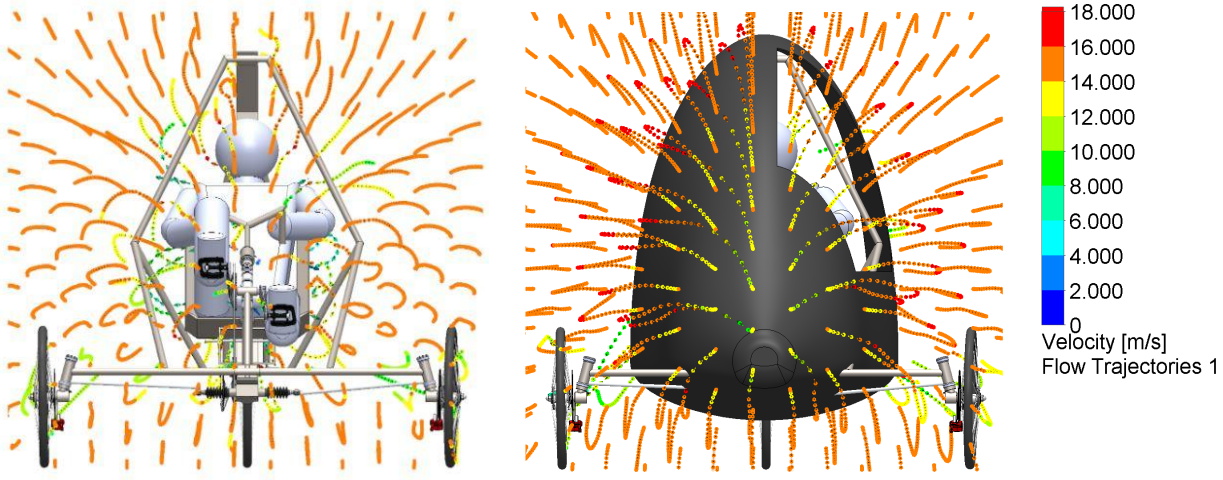

Figure 17. Air streamlines without (left) and with (right) the preliminary design of the fairing

Through CFD analysis, it was discovered that preliminary fairing concept designs had high-pressure areas around sharp edges and abrupt curves. These high-pressure areas greatly

contributed to the amount of drag force on the vehicle during forward movement. To mitigate these high-pressure points, edges were made were rounded and curves were made more gradual. After CFD analysis, it was determined that the drag force on the vehicle without the fairing is 55.3 N, while the drag force on the vehicle with the fairing is 31.8 N. The fairing reduced the drag on the vehicle by 42.5% at a constant velocity of 15 m/s. Because of this large reduction in drag and the little weight the fairing adds to the vehicle, the fairing was decided to be a necessary asset to the HPV.

However, in the preliminary stages of the manufacturing process, it was found that the fairing design shown in Figure 13 was going to be too difficult to manufacture, given the current resources and timeline. A simpler, less enclosed fairing was developed, as shown in the drawing view on page 2. Although no CFD was conducted on this new design, the team still believes that this fairing's effectiveness warrants the production of it.

2.4 Cost Analysis

Funding was requested from the University of Virginia's Mechanical Engineering Department, the Experiential Fund, and the Parents Fund at UVA. A total of $4218 was allocated to the team. Because of the ASME HPVC in-person cancellation due to COVID-19, all costs such as transportation and travel expenses have been cut from the initial budget. All funding received will be allocated solely to the material cost and fabrication of the HPV. The University of Virginia will provide all tools and machining equipment necessary to complete the fabrication and research of the HPV. No third party labor costs were necessary as all labor will be performed by the students in the University of Virginia's Human Powered Vehicle Team.

A large portion of the budget will be allocated solely to raw material costs. Steel tubing, steel plating, and carbon fiber sheeting will be the most significant raw material costs. Assembled bike parts are also estimated to consume a large portion of the budget and will be purchased through local bicycle shops. Overall the vehicle is estimated to cost around $2,469. This estimation is well under the funding that was received. A summarized breakdown of estimated costs based on current market prices for parts is displayed in Table 10 below.

Table 10. Subsystem Budget Breakdown: Budget needed by each subsystem to purchase every part needed for the HPV, and the total budget estimated.

Subsystem	Cost
Frame	$750
Brakes	$95
Wheels	$50
Steering	$250
Drivetrain	$350
Misc/Safety	$350
Fairing	$500
Tax (5.3%)	$124
Total Cost:	$2,469

2.5 Other Analysis

2.5.1 Biomechanics Analysis

The measurements of each potential driver were taken by the drivers and entered into the table below to find the average size of our driver. These measurements were used to help optimize the size of the vehicle, so that there was enough room for the largest driver, while also accommodating for the smallest driver. The adjustable seat points were also dependent on the measurements so that optimal leg lengths and hip angles were available to all drivers to maintain comfort.

Table 11: Important Measurements of Drivers

	Skyler	Ryder	Trevor	Kavi	Lauren	Riley	Joe	Average
Height (in)	69	76	72	70	67	74	76	72
Total Leg Length (in)	36	42	42	37	40	44	43	40.57
Hip to Knee Length (in)	18	23	21	20	20	21	20	20.43
Knee to Ankle Length (in)	18	21	20	18	17	23	21	19.71
Arm Length (in)	25	28	27	27	21	28	30	26.57

2.5.2 Gear Analysis

A gearing analysis was conducted on various chainring sizes, the internal hub, and sprockets to determine if the intended internal hub would meet the speed requirements stated in the competition. Equations from previous years and Sheldon Brown's gear calculator were used for the analysis. In the equations, G is the grade of the hill and that value is assumed at around 5%, W is the total weight of the vehicle and rider and is estimated around 250 lbs (113.4 kg), and the gear ratio variable is provided by the chainring to sprocket size ratio and Sheldon Brown's calculator. The drag coefficient was calculated in aerodynamics analysis and was determined to be 0.21. The frontal area of the bike was modeled at 0.685 m^2. The data from the analysis is shown in Table 12.

$$P_{needed} = (F_{air\ res} + F_{roll\ res} + F_{hill\ grav} + F_{efficiency}) * v_{min}^{\ gear\ ratio} \quad \text{[Eq. 2]}$$

$$F_{air\ res} = \tfrac{1}{2}\rho A C_d v^2 \quad \text{[Eq. 3]}$$

$$F_{roll\ res} = \mu N = \mu W cos(tan^{-1} G) \quad \text{[Eq. 4]}$$

$$F_{hill\ grav} = W sin(tan^{-1} G) \quad \text{[Eq. 5]}$$

$$F_{efficiency} = 0.95 * F_{applied} \quad \text{[Eq. 6]}$$

Figure 18. Equations for Power Generation. Power generation equations were conducted by previous HPVC teams at UVA (Baber et. al, 2020).

$$P_{applied} = (9.8\ \tfrac{m}{s^2})(81.6\ kg)(.17\ m)(6.3\ \tfrac{rad}{s}) = 856.5\ W$$

$$P_{needed} = (0.633 + 45.3 + 5.66 + 760) * (16/38)(0.53) = 181.11\ W$$

$$F_{air\ res} = 0.5(1.225\ \tfrac{kg}{m^3})(0.685\ m^2)(0.21)(2.68\ \tfrac{m}{s})^2 = 0.633\ N$$

$$F_{roll\ res} = (0.4)(113.4\ kg)cos(tan^{-1}0.05) = 45.3\ N$$

$$F_{hill\ grav} = (113.4\ kg)sin(tan^{-1}0.05) = 5.66\ N$$

$$F_{eff} = 0.95(9.8\,\frac{m}{s^2})(81.6\,kg) = 760\,N$$

Figure 19. Example calculations. An example using the 38T chainring and a 180 lb driver.

Table 12: Power Output and Speeds for the Internal Hub Setup based on Chainring Sizes

	Front Chainring Size				
	42T	40T	38T	36T	34T
Minimum Speed (60 rpm uphill)	6.7 mph	6.3 mph	6.0 mph	5.7 mph	5.4 mph
Power needed for traveling uphill (60 rpm)	163.86 W	172.06 W	181.11 W	191.18 W	202.42 W
Maximum Speed (120 rpm flat)	40.9 mph	38.9 mph	37.0 mph	35.0 mph	33.1 mph

All chainring sizes are shown to reach the minimum required speed, so the 38T chainring was chosen because last year's team had that left over for the current team to reuse. From the biomechanics research, it was determined that 60 rpm is an achievable and economical cadence for the average bike rider in an endurance challenge, thus the amount of power required to climb hills is achievable based on the conservative weight and sizing used in the calculations that are shown in Figure 16. Furthermore, 120 rpm is double the assumed average cadence, which is shown to be a safe assumption in biomechanics research.

2.5.3 Steering Analysis

A steering analysis was conducted based on the rack and pinion that is to be purchased, chosen Ackermann Angles, and the length of the tie rods connecting the rack and pinion to the wheel assembly. The online specifications for the rack and pinion specify it has a travel, the max length the rack can move when turned, of 4 inches from max right position to max left position. This results in a max two-inch travel of the rack from a center position. When the Solidworks assembly is positioned with the rack two inches to the right it yields tire angles, δ_0 and δ_1 (See Figure 16), of 22.5 and 30.1 degrees respectively from the straight line. Based on the formulas from Dale Thompson at the University of Alabama, see Figure 16) these wheel angles, when converted to radians, would yield a turning radius of ~4.5 meters exceeding the specifications set by ASME (Thompson 2009).

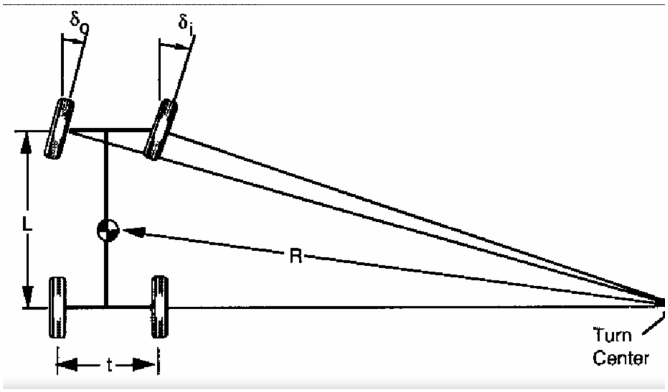

$$\delta_0 = \frac{L}{R+\frac{t}{2}}, \delta_1 = \frac{L}{R-\frac{t}{2}}$$

Figure 20. (left) Showing the geometric relationship that creates the turn center based on tire angles, (right) Equations that relate the tire angles with the turning radius of a vehicle

3 Conclusion

3.1 Evaluation

The primary objectives of the team are to design, develop, and build a human-powered vehicle that will meet the requirements of the ASME HPVC and will act as a practical alternative to combustion-powered vehicles. This entails prioritizing safety, reliability, and innovation in the design process. Each of the team's subgroups sought to actualize these goals through their research and development.

The central-spine frame design of the vehicle is an innovative concept in this particular application as most human-powered vehicles incorporate some sort of web design. This unique design allows for lighter overall weight and still provides extremely sturdy rollover protection with side and top deflections due to loading being well under what is required for the competition. Incorporating biomechanics research from peer-reviewed papers as well as scientific institutions informed many of our design choices to maximize the comfort of the driver as well as optimize the efficiency of the transfer of power from the driver to drive the vehicle. This research was pivotal and successful in making our design as practical and efficient as possible for the average, as well as a broad range, of potential drivers. The vehicle's drivetrain assembly involving petaled cranks that drive the rear wheel through two separate chains provides a unique solution to the potential problems that can arise from driving a wheel that is situated far away from where the power is being generated. The two chain solution successfully reduces the risks of slack or interference with other vehicle elements which are highly problematic when an overly long chain is used. In addition, the drivetrain includes an internal hub shifter which greatly enhances reliability, durability, and precision when shifting. These are immensely important qualities for a vehicle that is intended to be a practical and reasonable mode of transportation for the average person. The steering subsystem utilized a rack and pinion assembly with Ackermann Steering geometry as well as a kingpin inclination. While these methods and assemblies are not new, they provide easy to use, reliable, and durable steering which accomplishes our stated goal of practicality. The vehicle's braking system entails two disk brakes on the two front wheels. Incorporating disk brakes, which have a high level of reliability, and distributing braking force to two wheels ensures a high level of safety.

At the end of manufacturing for the year, the vehicle is welded so that it is structurally sound with only a few small welds left. Due to COVID delays the vehicle took slightly longer than intended to reach its current state, but overall the vehicle has been on track. Very soon, a driver will be able to sit in and drive the vehicle with the addition of a seat. All subsystems except for the fairing and the seat have been implemented on the vehicle and work as anticipated. Several lessons were learned in manufacturing, such as how the pipes expand and contract during welding or how a chain needs to be routed to a specific distance for ideal tensioning. All of these lessons have been recorded and saved for future teams to use in a separate Lessons Learned document.

3.2 Comparison

Table 13: Comparison of Team Design Specification and Analytical Performance Prediction

Competition Parameter	Parameter Value	Team's Design Specification	Analytical Performance Prediction

Braking Distance	6 meters from ≥25 km/h	5 meters from 25 km/h	Requires 535N of braking force
Stability	Travels straight 30 meters at 5-8 km/h	Same as competition requirements	Speed met based on gearing analysis, straight stability anticipated based on design
Rollover Protection	<5.1 cm of deflection for top load of 5340N, <3.8 cm of deflection for side load of 2670N	<4 cm deflection for top load case, <3 cm for side load case	.542 cm for top load and .665 cm for side load
Turning Radius	8 meters	>6 meters	~4.5 m
Weight	N/A	< 100 lbs.	<100 lbs is anticipated
Size	Fits tallest and shortest riders with >2” clearance between helmet and roll cage	Fits riders between 66” and 77” with >2” clearance	Model allows shortest and tallest riders with >2” clearance

3.3 Recommendations

The vehicle satisfies the requirements the team laid out. However, for future work, there are some improvements that could be made. The frame was over-designed and is much stronger and heavier than it needs to be. As far as manufacturing the frame, the most important aspect to pay attention to is warping while welding. Keeping the pipes attached to the MDF boards for as long as possible helps to minimize the warping. As far as the steering system, while over-seat steering worked for this vehicle, under-seat steering should be investigated as a potential alternate solution because it presents some advantages. For steering manufacturing, FEA could have been conducted on the steering assembly because the cantilevered axle that the wheel rests on may be over-built. For the fairing, the primary recommendations involve creating a design with more flexible dimensioning which would make for easier manufacturing. As far as biomechanics, even though the team’s design had a relative seat location, the exact specifications were not planned out. Planning out the exact seat placement and mounting angles would allow for easier manufacturing.

References

Albemarle County Board of Supervisors. (2020, October). *Climate Action Plan*. https://www.albemarle.org/home/showpublisheddocument?id=5432

Baber, T., Banskota, S., Blundin, E., Bonnin, R., Chang, C., DeAngelis, T., Jeong, M., Lapierre, J., Mahaffey, B., Matthews, C., Patterson, J., & Qi, H. (2020). *2020 ASME human-powered vehicle competition e-fest north* (Technical design report). The University of Virginia, Charlottesville, VA.

Baldissera P., Delprete C., Zahar A. (2019). Design and construction of a moving cassette electronic gear-shift for human-powered vehicles. *MDPI*. Retrieved from https://www.mdpi.com/2075-1702/7/3/55/htm

Beauchamp, W. (2018, October). The Recumbent & HPV Information Center. Retrieved January 19, 2021, from http://www.recumbents.com/home/

Cote, O., Fromm, D., Juri, M., Opitz, L. (2019). Final design report for human-powered vehicle drivetrain project. *Digital Commons @ Cal Poly.* Retrieved from https://digitalcommons.calpoly.edu/mesp/489/

Fisher, A., Sahyoun, A., Schmelzer, G., Taylor, B., Toy, C. (2015). One ride human-powered vehicle. *Santa Clara University Scholar Commons.* Retrieved from https://scholarcommons.scu.edu/cgi/viewcontent.cgi?article=1040&context=mech_senior

Gregor, S. M., Perell, K. L., Rushatakankovit, S., Miyamoto, E., Muffoletto, R., & Gregor, R. J. (2002). Lower extremity general muscle moment patterns in healthy individuals during recumbent cycling. Clinical Biomechanics, 17(2), 123-129.

Jong, P. (2006). Multi-body modeling of recumbent cycling: An optimization of configuration and cadence. Retrieved from file://Jong_2006_Multi-body%20modelling%20of%20recumbent%20cycling_An%20optimisation%20of%20configuration%20and%20cadence.pdf

LaFrance, A. (2019, December 28). Learn Camber, Caster, and Toe: Suspension Alignments. Retrieved January 09, 2021, from https://www.comeanddriveit.com/suspension/camber-caster-toe

Thompson, D. (2009, November 20). Ackermann? Anti-Ackermann? or Parallel? Retrieved January 10, 2021, from https://www.me.ua.edu/me364/PDF/Steering_Ackerman.pdf

Too, D., Landwer, G. (1993). The biomechanics of force and power production in human-powered vehicles. *Digital Commons @Brockport*. Retrieved from http://www.whpva.org/HParchive/hp55p3-6.pdf

Too, D., Landwer, G. (1993). Maximizing performance in human-powered land vehicles: a literature review and directions for future research. *Digital Commons @Brockport*. Retrieved from https://digitalcommons.brockport.edu/cgi/viewcontent.cgi?article=1102&context=pes_facpub

Why Use an Internal Gear Hub? (2015, October 23). Retrieved from https://www.montaguebikes.com/folding-bikes-blog/2011/05/why-use-an-internal-gear-hub/